JOURNAL OF AGRICULTURAL AND FOOD CHEMISTRY

Heat-Induced Changes in Myofibrillar Protein Structures and Myowater of Two Pork Qualities. A Combined FT-IR Spectroscopy and Low-Field NMR Relaxometry Study

HANNE CHRISTINE BERTRAM,*,† ACHIM KOHLER,‡ ULRIKE BÖCKER,‡ RAGNI OFSTAD,‡ AND HENRIK J. ANDERSEN†

Department of Food Science, Danish Institute of Agricultural Sciences, Research Centre Foulum, P.O. Box 50, DK-8830 Tjele, Denmark, and MATFORSK, Norwegian Food Research Institute, Osloveien 1, N-1430 Ås, Norway

Low-field NMR T_2 and Fourier transform infrared (FT-IR) measurements were performed on meat samples of two qualities (normal and high ultimate pH) during cooking from 28 °C to 81 °C. Pronounced changes in both T_2 relaxation data and FT-IR spectroscopic data were observed during cooking, revealing severe changes in the water properties and structural organization of proteins. The FT-IR data revealed major changes in bands in the amide I region (1700−1600 cm^{-1}), and a tentative assignment of these is discussed. Distributed NMR T_2 relaxation data and FT-IR spectra were compared by partial least-squares regression. This revealed a correlation between the FT-IR peaks reflecting β-sheet and α-helix structures and the NMR relaxation populations reflecting hydration water ($T_{2B} \sim 0-10$ ms), myofibrillar water ($T_{21} \sim 35-50$ ms), and also expelled "bulk" water (T_2 relaxation times >1000 ms). Accordingly, the present study demonstrates that definite structural changes in proteins during cooking of meat are associated with simultaneous alterations in the chemical−physical properties of the water within the meat.

KEYWORDS: Water distribution; muscle; protein denaturation; cooking; multivariate data analysis

INTRODUCTION

Fresh meat characteristics and cooking conditions, e.g. heating rate and temperature, are substantial for the sensory perception of meats (*1*−*7*). Consequently, a basic understanding of the physical−chemical properties of the myofibrillar matrix and belonging myowater, which constitute more than 95% of fresh meat, before and during heating is important both to elucidate and optimize perceived meat quality. This applies with special force in the production of convenience products and optimized formulation of restructured meat and fish products.

Meat proteins denature upon heating. This has been demonstrated in differential scanning calometry (DSC) studies on meat. These have revealed three denaturation steps that have been ascribed mainly to myosin denaturation (∼40−60 °C), sarcoplasmic protein and collagen denaturation (∼60−70 °C), and actin denaturation (∼80 °C) (*8*−*10*). However, while DSC enables detection of protein denaturation, this technique provides no information about the specific structural changes in the proteins during the denaturation process. In contrast, infrared (IR) spectroscopy measures fundamental molecular vibrations, which facilitate studies of the morphology and structure of proteins at the molecular level (*11*). Recently, Fourier transform IR (FT-IR) spectroscopy has been demonstrated both to be an appropriate tool in the prediction of WHC in pork (*12*) and to elucidate the oxidative stability in pork adipose tissue (*13*). Moreover, a recent study demonstrated the potential of Fourier transform IR (FT-IR) microscopy to elucidate heat-induced denaturation processes in beef (*14*).

The main constituent of fresh meat, water (70−75%), is mainly held within the highly organized structures of myofibrillar proteins (*15*). The myofibrillar proteins denature upon heating, and severe structural changes, that must be expected to affect the properties of the water within the meat (myowater), take place. Recently, it was demonstrated that changes in the chemical−physical properties of myowater (mobility and distribution of the water populations) can be studied continuously upon heating by low-field ^{1}H NMR T_2 relaxometry (*16*−*17*). Accordingly, the combination of FT-IR spectroscopy and low-field ^{1}H NMR T_2 relaxometry facilitates a simultaneous characterization of protein structures and myowater properties. The aim of the present study was to use the combination of FT-IR spectroscopy and low-field ^{1}H NMR T_2 relaxometry to characterize changes in myofibrillar protein structures and the chemical−physical properties of myowater upon heating of meat and the influence of fresh meat quality (normal and high ultimate pH of the fresh pork) on these changes.

MATERIALS AND METHODS

Meat and Sample Preparation. To obtain meat of two qualities, two slaughter pigs which were offspring of Duroc/Landrace boars

* To whom correspondence should be addressed. Phone: +45 89 99 15 06. Fax: +45 89 99 15 64. E-mail: HanneC.Bertram@agrsci.dk.
† Research Centre Foulum.
‡ Norwegian Food Research Institute.

10.1021/jf0514726 CCC: $33.50
Published on Web 02/07/2006

crossbred with Landrace/Yorkshire sows were included in the study. One of the pigs was injected with adrenaline (subcutaneous injection, 0.2 mg/kg live weight) 16 h before slaughter to increase the final pH of the meat as described previously (*18*). The pigs were slaughtered in the experimental abattoir at Research Centre Foulum. At the time of slaughter, the pigs had a live weight of approximately 100 kg. They were stunned by 80% CO_2 for 3 min, exsanguinated, and scalded at 62 °C for 3 min. Cleaning and evisceration of the carcasses were completed within 30 min post mortem. The carcasses were split and kept at 12 °C. Within 3 h post mortem, the carcasses were transferred to a chill room, where they were stored at 4 °C.

At 24 h post mortem, pH was measured at the last rib curvature of *M. longissimus dorsi*. The measurements were carried out with a pH meter (Metrohm AG CH 9101, Herisau, Switzerland). The calibration temperature was 4 °C, and a two-point calibration was carried out using calibration buffers with pH 7.000 and 4.005 at 25 °C (Radiometer, Copenhagen, Denmark). The pH values in the two obtained meat qualities, "normal ultimate pH" and "high ultimate pH", were 5.4 and 6.5, respectively.

At 24 h post mortem, two ∼5 cm broad chops were cut from the middle of *M. longissimus dorsi* from the right side of each carcass. From each chop, a total of 10 samples were cut (∼3.5 cm long and 1 × 1 cm^2 in sectional area, weight ∼3−4 g) along the fiber direction and placed vertically in a cylindrical glass tube with a plastic lid. After samples were heated to 10 various temperatures (28.5, 34.0, 40.0, 46.1, 52.0, 57.6, 63.0, 69.3, 75.5, and 81 °C), NMR measurements were performed on the samples (see below) at a temperature identical to the sample temperature. Subsequently, two blocks (5 × 5 × 2 mm^3) were excised from each sample used for NMR measurements and embedded in O.C.T. compound (Tissue-Trek, Electron Microscopy Sciences, Hatfiles, USA), immediately frozen in liquid nitrogen and stored at −80 °C prior to sectioning. Sectioning was carried out at −22 °C, transversely to the fiber direction. A cryostat (Leica CM 3050 S, Nussloch, Germany) was used, and 8 μm thick sections were prepared and thaw-mounted on infrared transparent, 2 mm thick CaF_2 slides for FT-IR microscopic measurements.

NMR Measurements. The NMR ^1H T_2 relaxation measurements were performed on a Maran benchtop pulsed NMR analyzer (Resonance Instruments, Witney, U.K.) with a resonance frequency for protons of 23.2 MHz and equipped with an 18 mm temperature variable probe. Transverse relaxation times (T_2) were measured using the Carr−Purcell−Meiboom−Gill (CPMG) sequence. The T_2 measurements were performed with a τ-value (time between the 90° pulse and the 180° pulse) of 150 μs and using a relaxation delay of 3 s, and data were acquired as the amplitude of every second echo (to avoid the influence of imperfect pulse settings) in a train of 4096 echoes (only the even-numbered echoes were used in the data analysis). A total of 16 scans were accumulated. The NMR measurements were carried out on two samples at each of the 10 temperatures mentioned above; however, only one measurement was carried out at 28.5 °C for the normal ultimate pH meat, resulting in 39 relaxation curves.

Distributed exponential fittings of CPMG decay curves (*19*) were performed in Matlab (The Mathworks Inc., Natick, MA) using in-house scripts. The data were pruned from 2048 to 256 points using linear pruning, which on synthetic data was found to give robust solutions. This analysis resulted in a plot of relaxation amplitude for individual relaxation processes versus relaxation time.

FT-IR Microspectroscopy. An IR microscope (IRscope II) coupled to an Equinox 55 FT-IR spectrometer (both Bruker Optics, Germany) was used to measure the tissue sections. The microscope was equipped with a computer-controlled *x*,*y* stage. The Bruker system was controlled with an IBM-compatible PC running OPUS-NT software, version 4.0. IR spectra were collected from single myofibers (30−60 μm in diameter depending on the heat treatment) in transmission mode from 4000 to 700 cm^{-1} with a spectral resolution of 6 cm^{-1} using a mercury-cadmium-tellurium (MCT) detector. Three spectra were acquired from one section per block obtained from the samples used for NMR measurements as described above. For each spectrum 256 interferograms were coadded and averaged. The microscope, which was sealed using a specially designed box, and the spectrometer were purged with dry air to reduce spectral contributions from water vapor and CO_2. A background spectrum of the CaF_2 substrate was recorded before each sample measurement in order to account for variations in water vapor and CO_2 levels.

Preprocessing of FT-IR Spectra. The FT-IR spectra of the myofibers showed a strong day-to-day variation due to varying water content in the sections used for microscopy, presumably due to variations in the flushing of the FT-IR microscope with dry air. To remove the variation owing to differences in water content in the sections, extended multiplicative signal correction (EMSC) was used (*20*, *21*). In the basic form of EMSC, every spectrum $z(\tilde{\nu})$, where $\tilde{\nu}$ is the wavenumber and defined as the reciprocal of the wavelength λ, is written as

$$z = a + bm + d\tilde{\nu} + e\tilde{\nu}^2 + \sum_{j=1}^{J-1} h_j \Delta k_j + \epsilon_i \qquad (1)$$

a linear combination of a baseline shift a, a multiplicative effect b times a reference spectrum m, linear and quadratic wavenumber-dependent effects $d\tilde{\nu}$ and $e\tilde{\nu}^2$, respectively, and $J - 1$ difference spectra of constituent spectra $\Delta k_j(\tilde{\nu})$ times parameters h_j. The $J - 1$ constituent difference spectra $\Delta k_j(\tilde{\nu})$ are defined as the differences between J known constituent spectra. The parameters h_j are defined as $h_j = b\Delta c_j$, with $\Delta c_j = c_j - c_j^m$, where c_j and c_j^m are the concentrations of the constituent spectra $k_j(\tilde{\nu})$ in the spectrum $z(\tilde{\nu})$ and the reference spectrum m, respectively. The term ϵ contains the unmodeled residuals. The EMSC parameters a, b, d, e, and h_j are estimated by ordinary least squares. To remove the contribution in spectra due to variations in flushing, an additional experiment was run, where we acquired spectra from one single myofiber and systematically changed the water amount in the section by increasing the flushing time. One difference spectrum $\Delta k_j(\tilde{\nu})$ was then calculated as the difference between spectra for different levels of flushing (from the same myofiber). After the estimation of the EMSC parameters, the spectra $z(\tilde{\nu})$ were then corrected according to

$$z_{corr} = (z - a - d\tilde{\nu} - e\tilde{\nu}^2 - h_j \Delta k_j)/b \qquad (2)$$

After EMSC the second derivative of the spectra was taken in order to resolve nearby lying bands. After preprocessing, the spectra from the same block (see above) were averaged. Averaging resulted in 40 spectra in total from the two animals (normal and high ultimate pH), 10 different temperatures, and 2 parallel blocks for each sample.

Multivariate Analysis. To estimate a correlation between the design variables temperature and meat quality ("normal ultimate pH" and "high ultimate pH"), FT-IR absorbances, and variables obtained by NMR spectroscopy, we used partial least squares regression (PLSR). In PLSR the response variables **Y** (e.g. FT-IR spectra of N samples with K_2 variables) are expressed as a linear function of the variables **X** (e.g. NMR spectra of N samples with K_1 variables)

$$\mathbf{Y} = \mathbf{B_0} + \mathbf{XB} + \mathbf{F} \qquad (3)$$

where $\mathbf{B_0}$ is the $N \times K_1$ matrix of offsets with identical values in every column (every variable has the same offset for all samples N), **B** is the matrix of regression coefficients with $K_1 \times K_2$ entries, and **F** the $N \times K_2$ matrix of residuals (*22*). **X** is transferred to a new coordinate space, where the new "latent **X**-variables", the so-called scores, have a diagonal covariance matrix. The directions in this new coordinate space are given by the loading vectors (as a function of the old variables). In addition, the new variables are ordered according to the magnitude of their covariance to **Y**; that is, the first PLS component contains the largest covariance and so on.

To visualize the correlation between design, FT-IR, and NMR variables, so-called correlation loading plots are used. In a correlation loading plot, *x*- and *y*-loadings are scaled in such a way that they can be displayed in the same plot. The correlation loading plot shows then the correlation of both *x*- and *y*-variables to the corresponding PLS components. This allows us to study the correlation between *x*- and *y*-variables. For investigation of the effect of the design on the FT-IR and NMR variables, the design variables were used as **X** and the FT-

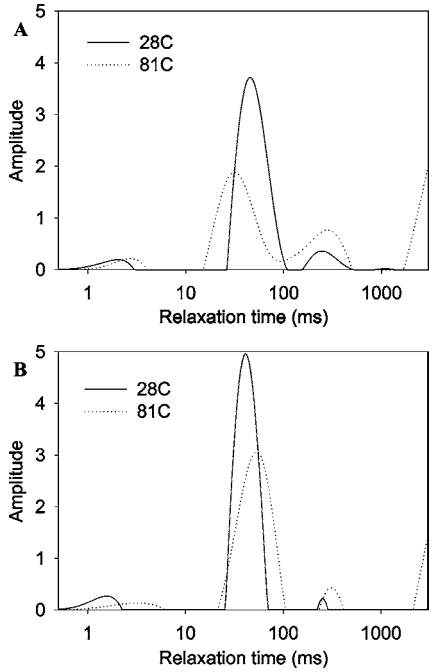

Figure 1. Distribution of NMR T_2 relaxation times in pork with (A) normal ultimate pH and (B) high ultimate pH at 28 and 81 °C.

IR or NMR variables as **Y** in PLSR. In this case the 10 temperatures are defined as so-called indicator variables, where each temperature is expressed by a variable with the value 0 or 1, indicating if the samples were treated with the respective temperature or not. The same applies for the normal and high ultimate pH. The design, FT-IR, and NMR variables were weighted by their standard deviations prior to PLSR. The data analysis was performed using Unscrambler version 9.1 (Camo AS, Oslo, Norway, 2004), by algorithms written in Matlab and by in-house-developed algorithms written in C++.

RESULTS

NMR Measurements. Parts **A** and **B** of **Figure 1** show the distributed T_2 relaxation times measured at 28 and 81 °C for the meat with normal and high ultimate pH, respectively. In the nonheated meat (28 °C), three relaxation populations centered at approximately 0−10, 35−50, and 200−400 ms (designated T_{2B}, T_{21}, and T_{22}, respectively) were observed. Upon heating (81 °C), a marked broadening of the populations centered at 35−50 (T_{21}) and 200−400 ms (T_{22}) was evident. Moreover, upon heating, a relaxation population with relaxation times > 1000 ms corresponding to expelled bulk water was detected. Both in the nonheated meat and especially upon heating, the relaxation populations centered at 35−50 (T_{21}) and 200−400 ms (T_{22}) were clearly broadened in the meat with normal ultimate pH compared with meat with high ultimate pH. Moreover, upon heating, the T_{2B} relaxation population moved from approximately 0−2.5 ms to approximately 2.5−10 ms in both meat qualities. Parts **A** and **B** of **Figure 2** display contour plots of the magnitude of distributed NMR T_2 relaxation times as a function of heating temperature for the meat with normal ultimate and high ultimate pH, respectively. While the meat with high ultimate pH is characterized by three distinct relaxation populations during the entire heating course (**Figure 2B**), a marked broadening of the relaxation populations is observed in meat with normal ultimate pH (**Figure 2A**) during heating, and around 50 °C the populations centered at 35−50 (T_{21}) and 200−400 ms (T_{22}) merge, and they blur steadily with increasing temperatures. The correlation plot (for the first and

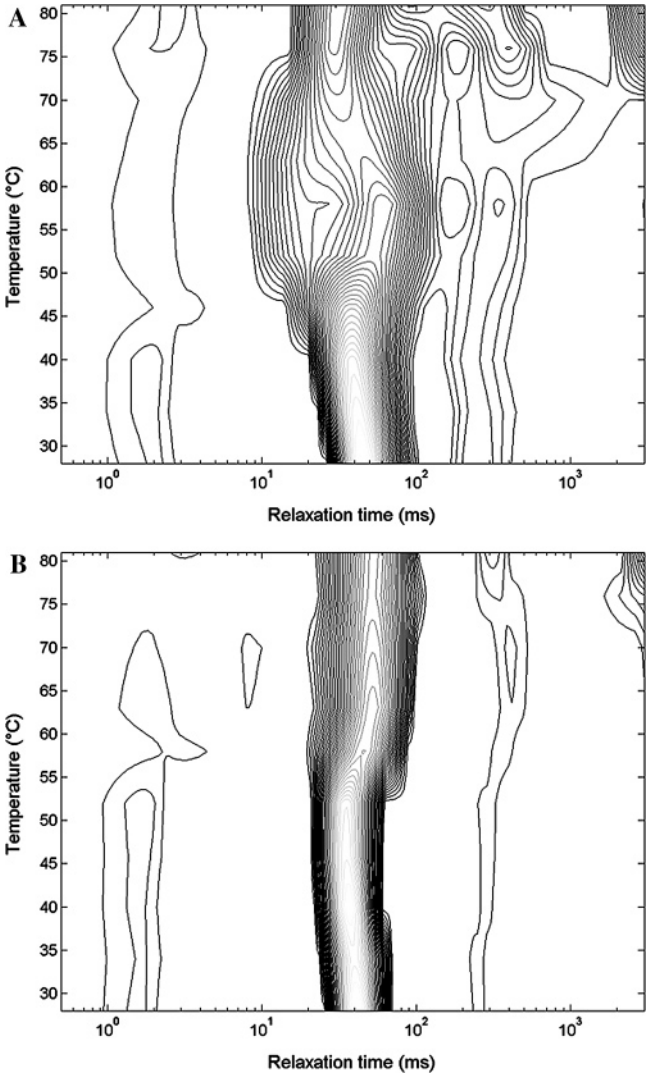

Figure 2. Contour plot of distributed exponential fitting of T_2 relaxation upon heating (28–81 °C) of pork samples with (A) normal ultimate pH and (B) high ultimate pH. During cooking a broadening of the major population around 30–80 ms is observed, and above 70 °C, expelled water with relaxation times > 1000 ms appears.

second PLS components) of the PLSR with design of the experiment as X and the distributed T_2 relaxation times as Y is shown in **Figure 3**. The range of relaxation times between 0 and 2.5 ms as well as between 35 and 50 ms, corresponding to T_{2B} and T_{21}, respectively, is positively correlated toward low temperatures (28.5−52 °C) and high ultimate pH. The range of relaxation times between 200 and 400 ms as well as between 1000 and 3000 ms, corresponding to T_{22} and expelled water, respectively, is positively correlated toward high temperatures (57.6−81 °C) and normal ultimate pH.

FT-IR Microspectroscopy. Figure 4 shows the second derivative of the FT-IR spectra of meat with normal pH in the amide I region (1700−1600 cm^{-1}) for the 10 different temperatures. Prior to taking the second derivative, the spectra were preprocessed by EMSC as described above. The minima in the second derivatives refer to maxima (bands) in the original spectra. In **Figure 4** we are able to identify nine bands at the wavenumbers 1695, 1682, 1668, 1660, 1652, 1639, 1628, 1619, and 1610 cm^{-1}. All these bands have very strong correlation to the temperature used for the heat treatment. The bands at 1695, 1668, 1628, and 1619 cm^{-1} all have positive correlations toward

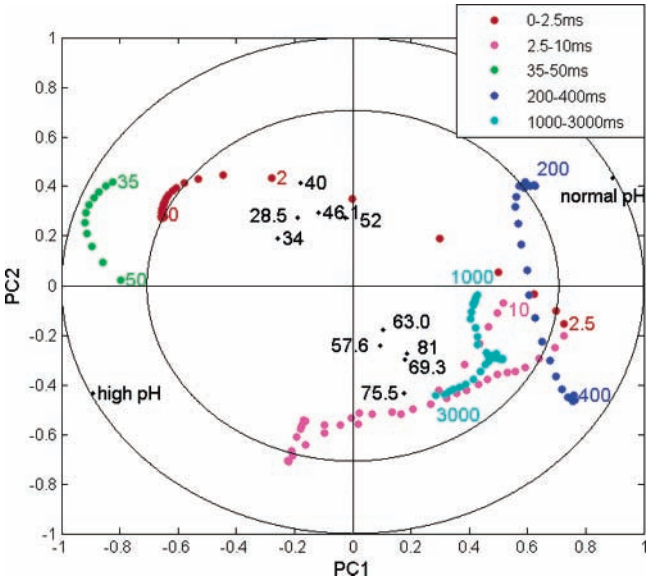

Figure 3. Correlation loading plot (first and second PLS components) of PLSR with the design (temperature and pH) as *X* and NMR data as *Y*. The validated explained variances are 15%/11% for *X* and 33%/11% for *Y*, for the first and second components, respectively. The inner and outer ellipses refer to 50% and 100% explained variance in *X* and *Y*, respectively.

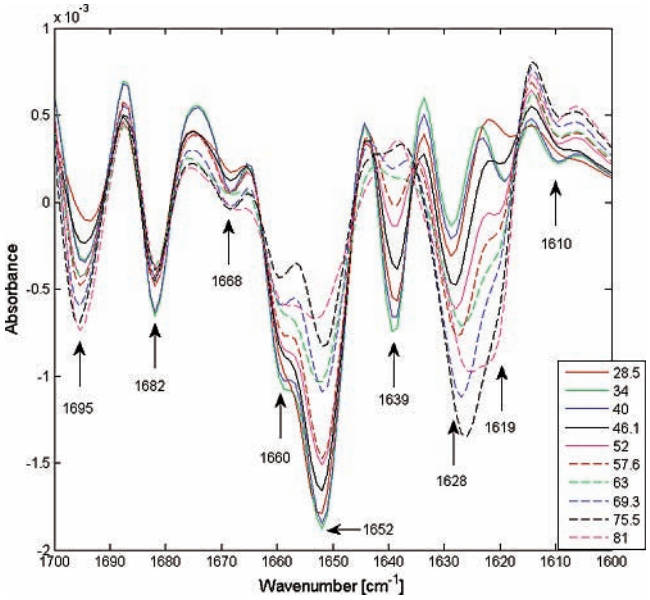

Figure 4. Seconnd derivative of the FT-IR spectra of meat with normal pH in the amide I region (1700–1600 cm^{-1}) for the 10 different temperatures.

temperature. As an example, the 1695 cm^{-1} band is plotted as a negative second derivative against the temperature for the mean spectra of every section in **Figure 5A**. The bands at 1682, 1660, 1652, 1639, and 1610 cm^{-1} all have negative correlations toward temperature, and as an example, the 1652 cm^{-1} band is plotted as the negative second derivative against the temperature for the mean spectra of every section in **Figure 5B**. These correlations are confirmed in the correlation loading plot (for the first and second PLS components) of the PLSR with design of the experiment as *X* and the nine absorbances (second derivative after EMSC) as *Y* in **Figure 6**. We see again that the absorption bands at 1695, 1668, 1628, and 1619 cm^{-1} are positively correlated toward high temperatures (55.6−81 °C)

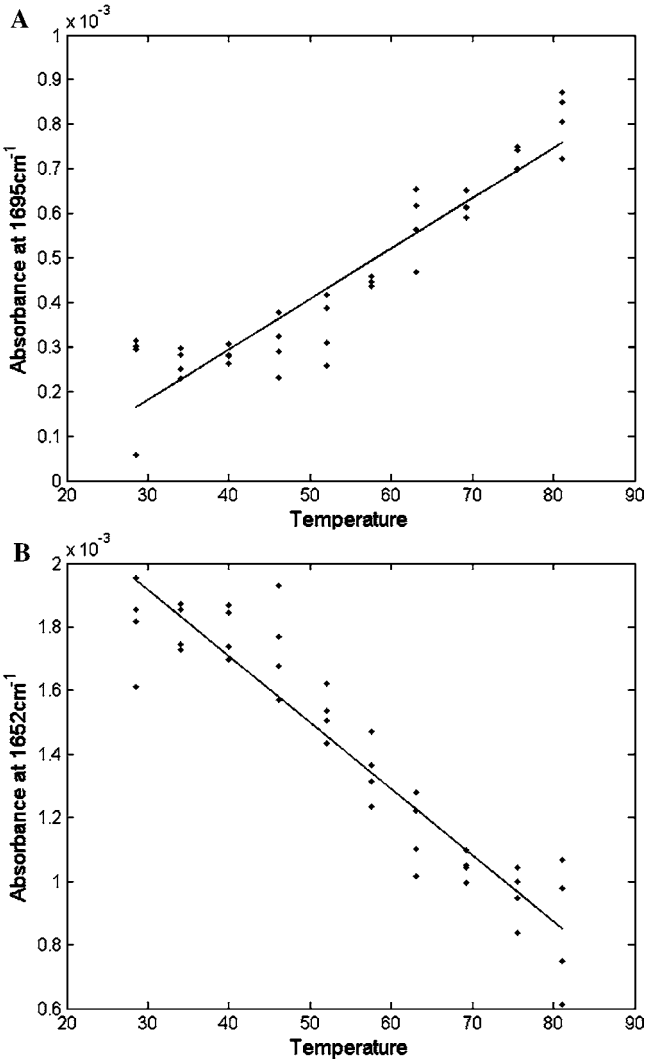

Figure 5. (**A**) The 1695 cm^{-1} band and (**B**) the 1652 cm^{-1} band (negative second derivative) plotted against temperature.

and the bands at 1682, 1660, 1652, 1639, and 1610 cm^{-1} are positively correlated toward low temperatures (28.5−52 °C). No significant correlation was observed between pH and the selected FT-IR variables.

Comparison of FT-IR and NMR Data. Figure 7 shows the correlation loading plot with the T_2 variables as *X* and the nine selected variables from FT-IR as *Y* (negative second derivative after EMSC as described above). There are positive correlations between FT-IR absorbance variables 1695, 1668, 1628, and 1619 cm^{-1} and the NMR variables in the ranges 2.5−10 ms (T_{2B}, bound water) and 200−400 ms (T_{22}, water located outside the myofibrillar protein network) and 1000−3000 ms (expelled bulk water). There is a positive correlation between the FT-IR absorbance variables 1682, 1660, 1652, 1639, and 1610 cm^{-1} and the NMR T_2 variables 0−2 ms (T_{2B}, bound water) and 35−50 ms (T_{21}, water trapped within the protein-dense myofibrillar network). For the T_2 variables 2−2.5 ms, a shift from the right to the left in the correlation loading plot is visible.

DISCUSSION

Heating of meat is associated with thermal denaturation of the myofibrillar proteins and a simultaneous change in the binding of water, which is reflected in loss of water. However, at present, the relationship between heat-induced changes in the

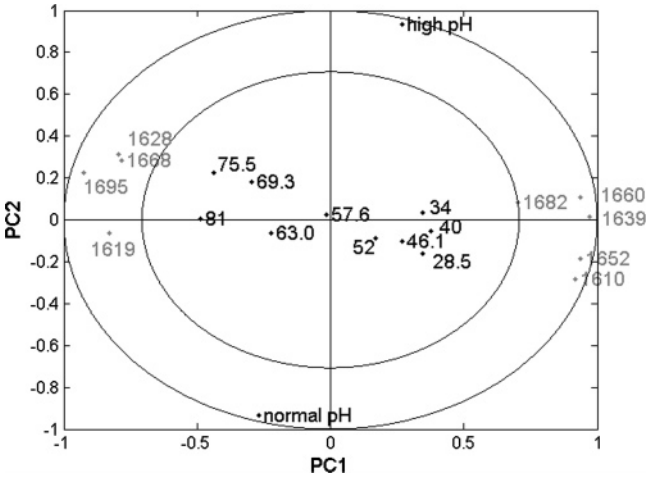

Figure 6. Correlation loading plot (first and second PLS components) of ANOVA PLSR with the design (temperature and pH) as *X* and selected variables of the (negative) second derivative of the amide I region of the FT-IR spectra as *Y*. The validated explained variances are 10%/16% for *X* and 76%/4% for *Y*, for the first and the second components, respectively. The inner and outer ellipses refer to 50% and 100% explained variance in *X* and *Y*, respectively.

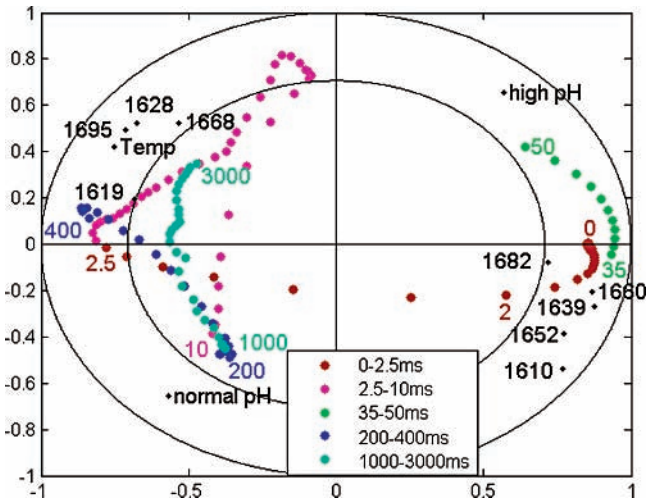

Figure 7. Correlation loading plot (first and second PLS components) of PLSR2 with distributed NMR variables as *X* and the (negative) second derivative of the amide I region of the FT-IR spectra as *Y*. The validated explained variances are 39%/13% for *X* and 55%/15% for *Y* for the first and second components, respectively.

highly organized protein structures and heat-induced changes in water distribution in the meat is still an almost unexplored area. In the present study FT-IR spectroscopy and low-field ^{1}H NMR T_2 relaxometry were for the first time combined to facilitate a simultaneous characterization of protein structures and myowater properties during heating. During heating, marked changes in the NMR T_2 relaxation characteristics were observed, corresponding to alterations in water properties. The heat-induced changes in the distributed T_2 data were characterized by a broadening of the water population representing myofibrillar water, which most probably reflects the formation of an amorphous myosin gel consisting of pores with a continuum of sizes, as also described earlier (*16*, *17*).

Applying FT-IR spectroscopy, the amide I region (1700−1600 cm^{-1}) was used in the characterization of changes in protein secondary structures during heating. The amide I region is dominated by carbonyl stretching vibrations with minor contributions from C−N stretching and N−H bending. A tentative assignment of the nine bands (1695, 1682, 1668, 1660, 1652, 1639, 1628, 1619, 1610 cm^{-1}) in the amide I region (1700−1600 cm^{-1}), found to change during heating, is discussed in the following.

The band at 1652 cm^{-1}, which is found to decrease with increasing temperatures, is most likely referring to the C═O bond in an α-helical structure of myofibrillar proteins (*23*). This decrease can be explained by splitting of the band caused by transition dipole coupling when either intramolecular or intermolecular peptides approach each other (*24*). This splitting of the amide I band can be as large as about 60 cm^{-1}, and the strength of the splitting basically depends on the distance of the C═O bonds of the different chains (*25*). Taking into consideration the correlation between the absorption bands and the temperatures used for the heat treatment, we tentatively assign the bands at 1695 cm^{-1} (high frequency) and 1619/1628 cm^{-1} (low frequency) to aggregated β-strands (intermolecular dipole coupling) and those at 1682 cm^{-1} (high frequency) and 1639 cm^{-1} (low frequency) to native β-sheet structures (intramolecular) (*23*). Around 1640 cm^{-1}, we also expect a band from the O−H bending of water. Therefore, care has to be taken in the interpretation of this band (*26*). Like the band at 1652 cm^{-1}, arising from α-helical structures, the absorption band at 1660 cm^{-1} is also decreasing with increasing temperature. It is therefore very likely that also this band is referring to native structures, probably loops in native structures that are expected to appear in this region (*23*). The weak absorption band at 1668 cm^{-1} increases significantly at higher temperatures with a critical point at 57.6 °C, after which the increase gathers momentum. This might indicate incipient denaturation of a specific protein; however, we have currently no explanation for this band. The weak band at 1610 cm^{-1} is increasing with increasing temperature and may tentatively be assigned to the amino acid side chain in tyrosine (*23*).

The information about protein structure as assessed by FT-IR spectroscopy can be correlated to the NMR measurements by comparison of the two data sets. PLS regression using the selected NMR T_2 variables as *X* and selected negative second derivative FT-IR variables as *Y* enables us to investigate covariances in both data sets. In the corresponding correlation loading plot (**Figure 7**), different regions in the NMR relaxation variables are colored differently, and certain NMR relaxation times are explicitly given in the plot. It can be seen that tightly bound water (T_{2B}, 0−2 ms, red) has a positive correlation to changes in intramolecular antiparallel β-sheets and α-helical structures. Myofibrillar-entrapped water (T_{21}, 35−50 ms, green) has a positive correlation to intramolecular antiparallel β-sheets and α-helical structures. Thus, water trapped within the highly dense and structured protein network is positively correlated to intramolecular antiparallel β-sheets and α-helical structures. It is important to point out that the band at 1639 cm^{-1} may also be due to water remaining in the tissue sections after drying (*26*). This strengthens the observations done by the NMR T_{2B} and T_{21} populations but weakens the evidence of the presence of intramolecular native β-sheets. T_{22} is increasing with increasing temperatures, and the positive correlations between T_{22} (200−400 ms, blue) and the FT-IR bands at 1695, 1628, and 1619 cm^{-1} reveal that an increase of aggregated structures leads to an increase of water located outside the myofibrillar protein network. As the amount of extramyofibrillar water has been shown to determine the amount of drip loss (*27*), this finding indicates that this type of protein structure is associated with a

reduced ability of the meat to retain water. Accordingly, a further elucidation of these IR bands is of great interest for understanding the role of this protein structure in relation to the water-holding capacity of the meat and meat products.

Finally, the distributed T_2 relaxation data show appearance of a water population with relaxation times above 1000 ms at higher temperatures, corresponding to expelled water. Correlations between this expelled water and FT-IR regions ascribed to thermally aggregated structures were demonstrated and imply that heat-induced changes in these structures are involved in the expulsion of water and formation of cooking loss.

Several studies have demonstrated that a high ultimate pH is associated with an improved water-holding capacity of meat (*18*, *28*−*30*) and a reduced cooking loss from meat (*31*−*33*). In the present study, NMR data demonstrated that a high ultimate pH has pronounced effects on water distribution. For the FT-IR spectra in the region 1700−1600 cm^{-1}, no significant effect of pH was observed. The reason for this may be that the effect of the secondary protein structure due to heat denaturation is much stronger than the effect of the pH and therefore difficult to confirm in the statistical analysis. This may indicate that pH variations between 5.4 and 6.5 of the raw material do not affect the protein secondary structure of the hand-treated meat. Further studies are needed to support the present findings.

ACKNOWLEDGMENT

Marianne Rasmussen and Vibeke Høst are appreciated for technical assistance.

LITERATURE CITED

(1) Aaslyng, M. D.; Bejerholm, C.; Ertbjerg, P.; Bertram, H. C.; Andersen, H. J. Cooking loss and juiciness of pork in relation to raw meat quality and cooking procedure. *Food Qual. Pref.* **2003**, *14*, 277−288.

(2) Bejerholm, C.; Aaslyng, M. D. The influence of cooking technique and core temperature on results of sensory analysis of pork-depending on the raw meat quality. *Food Qual. Pref.* **2003**, *15*, 19−30.

(3) Bertram, H. C.; Aaslyng, M. D.; Andersen, H. J. Elucidation of the relationship between cooking temperature, water distribution and sensory properties of pork − a combined NMR and sensory study. *Meat Sci.* **2005**, *70*, 75−81.

(4) Bowers, J. A.; Craig, J. A.; Kropf, D. H.; Tucker, T. J. Flavour, colour and other characteristics of beef longissimus muscle heated to seven internal temperatures between 55 °C and 85 °C. *J. Food Sci.* **1987**, *52*, 533−536.

(5) Heymann, H.; Hedrick, H. B.; Karrasch, M. A.; Eggeman, M. K.; Ellersieck, M. R. Sensory and chemical characteristics of fresh pork roasts cooked to different centre temperatures. *J. Food Sci.* **1990**, *55*, 613−617.

(6) Joseph, J. K.; Awosanya, B.; Adeniran, A. T.; Otagba, U. M. The effect of end-point internal cooking temperatures on the meat quality attributes if selected Nigerian poultry meats. *Food Qual. Pref.* **1997**, *8*, 57−61.

(7) Wood, J. D.; Nute, G. R.; Fursey, G. A.; Cuthbertson, A. The effect of cooking conditions on the eating quality of pork. *Meat Sci.* **1995**, *40*, 127−135.

(8) Wright, D. J. Differential scanning calorimetry -its application to the study of meat proteins. *J. Sci. Food Agric.* **1978**, *29*, 1088−1088.

(9) Stabursvik, E.; Martens, H. Thermal denaturation of proteins in post rigor muscle tissue as studied by differential scanning calorimetry. *J. Sci. Food Agric.* **1980**, *31*, 1034−1042.

(10) Stabursvik, E.; Fretheim, K.; Frøystein, T. Myosin Denaturation in Pale, Soft, and Exudative (PSE) Porcine Muscle Tissue as Studied by Differential Scanning Calorimetry. *J. Sci. Food Agric.* **1984**, *35*, 240−244.

(11) Thygesen, L. G.; Løkke, M. M.; Micklander, E.; Engelsen, S. B. Vibrational microspectroscopy of food. Raman vs. FT-IR. *Trends Food Sci. Technol.* **2003**, *14*, 50−57.

(12) Pedersen, D. K.; Morel, S.; Andersen, H. J.; Engelsen, S. B. Early prediction of water-holding capacity in meat by multivariate vibrational spectroscopy. *Meat Sci.* **2003**, *65*, 581−592.

(13) Guillén, M. D.; Cabo, N. Study of the effects of smoke flavourings on the oxidative stability of the lipids of pork adipose tissue by means of Fourier transform infrared spectroscopy. *Meat Sci.* **2004**, *66*, 647−657.

(14) Kirschner, C.; Ofstad, R.; Skarpeid, H.-J.; Høst, V.; Kohler, A. Monitoring of denaturation processes in aged beef loin by FT-IR microspectroscopy. *J. Agric. Food Chem.* **2004**, *52*, 3920−3929.

(15) Offer, G.; Knight, P. The structural basis of water-holding in meat, part 2: drip losses. In *Developments in meat science*; Lawrie, R., Ed.; Elsevier Applied Science: London, 1988; pp 172−243.

(16) Micklander, E.; Peshlov, B.; Purslow, P. P.; Engelsen, S. B. NMR cooking: The multiple states of water in meat during cooking. *Trends Food Sci. Technol.* **2002**, *13*, 341−346.

(17) Bertram, H. C.; Engelsen, S. B.; Busk, H.; Karlsson, A. H.; Andersen, H. J. Water properties during cooking of pork studied by low-field NMR relaxation: effects of curing and the RN-gene. *Meat Sci.* **2004**, *66*, 437−446.

(18) Henckel, P.; Karlsson, A.; Oksbjerg, N.; Petersen, J. S. Control of post mortem pH decrease in pig muscles: experimental design and testing of animal models. *Meat Sci.* **2000**, *55*, 131−138.

(19) Kroeker, R. M.; Henkelman, R. M. Analysis of biological NMR relaxation data with continuous distributions of relaxation times. *J. Magn. Reson.* **1986**, *69*, 218−235.

(20) Martens, H.; Stark, E. Extended multiplicative signal correction and spectral interference subtraction − new preprocessing methods for near-infrared spectroscopy. *J. Pharm. Biomed. Anal.* **1991**, *9*, 625−635.

(21) Kohler, A.; Kirschner, C.; Oust, A.; Martens, H. Extended Multiplicative Signal Correction as a tool for separation and characterisation of physical and chemical information in FT-IR microscopy images of cryo-sections of beef loin. *Appl. Spectrosc.*, **2005**, *59*, 707−716.

(22) Martens, H.; Næs, T. Extended multiplicative signal correction and spectral interference subtraction—new preprocessing methods for near-infrared spectroscopy. *Multivariate Calibration*; John Wiley & Sons: Chichester, U.K., 1989.

(23) Fabian, H.; Mäntele, W. Infrared Spectroscopy of Proteins. In *Handbook of Vibrational Spectroscopy*; Chalmers, J. M., Griffiths, P. R., Eds.; John Wiley & Sons Ltd: Chichester, U.K., 2002; pp 3399−3425.

(24) Barth, A.; Zscherp, C. What vibrations tell us about proteins. *Q. Rev. Biophys.* **2002**, *35*, 369−430.

(25) Krimm, S.; Bandekar, J. Vibrational Spectroscopy and Conformation of Peptides, Polypeptides, and Proteins. *Adv. Protein Chem.* **1986**, *38*, 181−364.

(26) Jackson, M.; Choo, L. P.; Watson, P. H.; Halliday, W. C.; Mantsch, H. H. Beware of connective tissue proteins: assignment and implications of collagen absorptions in infrared spectra of human tissues. *Biochim. Biophys. Acta* **1995**, *1270*, 1−6.

(27) Bertram, H. C.; Dønstrup, S.; Karlsson, A. H.; Andersen, H. J. Continuous distribution analysis of T_2 relaxation in meat—An approach in the determination of water holding capacity. *Meat Sci.* **2002**, *60*, 279−285.

(28) Bertram, H. C.; Whittaker, A. K.; Andersen, H. J.; Karlsson, A. H. pH-dependence of the progression in NMR T_2 relaxation times in post mortem muscle. *J. Agric. Food Chem.* **2003**, *51*, 4072−4078.

(29) Bertram, H. C.; Hu, J. Z.; Rommerein, D. N.; Wind, R. A.; Andersen, H. J. Dynamic High-Resolution ^1H and ^{31}P NMR Spectroscopy and ^1H T_2 Measurements in Postmortem Rabbit Muscles Using Slow Magic Angle Spinning. *J. Agric. Food Chem.* **2004**, *52*, 2681−2688.

(30) Bertram, H. C.; Whittaker, A. K.; Andersen, H. J.; Karlsson, A. H. The use of simultaneous ^{1}H & ^{31}P magic angle spinning nuclear magnetic resonance measurements to characterize energy metabolism during the conversion of muscle to meat. *Int. J. Food Sci. Technol.* **2004**, *39*, 661−670.

(31) Honikel, K. O. Vom Fleish zum Produkt. *Fleischwirtschaft* **2004**, *84*, 228−234.

(32) Mortensen, M.; Andersen, H. J.; Engelsen, S. B.; Bertram, H. C. Effect of freezing temperature, thawing and cooking rate on water distribution in two pork qualities. *Meat Sci.,* **2006**, *72*, 34−42.

(33) Zhang, S. X.; Farouk, M. M.; Young, O. A.; Wieliczko, K. J.; Podmore, C. Functional stability of frozen normal and high pH beef. *Meat Sci.* **2005**, *69*, 765−772.

Received for review June 22, 2005. Revised manuscript received December 1, 2005. Accepted December 8, 2005. We thank The Danish Ministry of Food, Agriculture and Fisheries for funding the project entitled "Characterisation of technological and sensory quality in foods", the Danish Research Council SJVF for funding the project "Characterization of basic NMR properties in perimortal muscles and meat in relation to physical and metabolic changes", and the Norwegian research council, who supported this study through Grant No. 15338/140.

JF0514726